ARTICLE IN PRESS

Nuclear Instruments and Methods in Physics Research A ■ (■■■■) ■■■–■■■

Contents lists available at ScienceDirect

Nuclear Instruments and Methods in Physics Research A

journal homepage: www.elsevier.com/locate/nima

Phase space analysis of secondary beams generated in hadron–photon collisions

C. Curatolo*, F. Broggi, L. Serafini

INFN Milan and University of Milan, via Celoria 16, Milan, Italy

ARTICLE INFO

Article history:
Received 25 May 2016
Accepted 1 September 2016

MSC:
00-01
99-00

Keywords:
Hadron–photon collider
Muon beam
Muon collider

ABSTRACT

Present availability of high brilliance photon beams in combination with intense TeV hadron beams makes it possible to conceive the generation of low emittance TeV-class energy pion/muon beams via photoproduction in a highly relativistic Lorentz boosted frame. We analyze the secondary beams brightness achievable by the coupling of advanced high efficiency high repetition rate FEL pulses and Large Hadron Collider or Future Circular Collider hadron beams. The phase space distributions of the pion and muon beams are obtained by means of an event generator code and the characteristics, such as emittance and energy spread, are benchmarked against analytical expressions.

1. Hadron–photon collider

Muon colliders represent a promising way to achieve the highest lepton–antilepton collision energies and precision measurements of the Higgs boson and for further study of its properties. Moreover, muons are ideal sources for neutrino beams of unprecedented quality and precision through their purely leptonic decay [1,2]. One of the main challenges of present muon collider design studies is the capture and cooling stage of muons after generation by intense GeV-class proton beams impinging on solid targets: this mechanism produces pions further decaying into muons and neutrinos. The large emittance of the generated pion beams, which is mapped into the muon beam, is mainly given by the mm-size beam source at the target and by Coulomb scattering of protons and pions propagating through the target itself, inducing large transverse momenta which in turns dilute the phase space area [3,4]. We propose an approach based on the collision of two counter-propagating beams of highly relativistic protons (LHC/FCC) and ultra-high brilliance FEL X-rays. The extremely high luminosity achievable by such a Hadron–Photon Collider (HPC) of about $10^{38}\ \mathrm{cm}^{-2}\ \mathrm{s}^{-1}$ can compensate for the low efficiency of the pion/muon photoproduction. There are two crucial aspects in such a collision scheme. The first is the much higher energy of the X-ray photons observed by the proton in its own rest frame: this enables pion photoproduction above the threshold with maximum efficiency, despite the keV energy of the colliding photon. The second deals with the proton carrying almost the total momentum of the system, which makes it the source of highly Lorentz boosted secondary beams collimated within a narrow forward angle of the same order of the proton beam diffraction angle given by its transverse emittance (tens of mm mrads). We considered two examples of TeV proton beams: an upgraded LHC [5] beam carrying up to $2\cdot 10^{11}$ protons per bunch at 7 TeV energy focused down to 7 μm at the interaction point with a normalized transverse emittance $\epsilon_{nx} = 1.4$ mm mrad and an FCC [6] expected beam at the same bunch intensity with 50 TeV energy, a spot size of 1.6 μm and $\epsilon_{nx} = 2.2$ mm mrad, both with a repetition rate up to 40 MHz. Photon beams at energies ranging between 3 keV and 20 keV and more than 10^{13} photons per pulse at MHz repetition rate can be obtained with SC-CW Linac based FELs, in saturation regime for the energies lower than few keV and in the tapering mode for larger energies [7,8]. In the next section we go through the details of the muon photoproduction, while the flux of the emitted particles is discussed in the dedicated section.

2. Pion/muon photoproduction

Let us consider the collision between a proton and a counter-propagating photon of energy respectively E_p and $h\nu$ in the laboratory frame (LAB). The energy $h\nu'$ of the colliding photon in the proton rest frame is given by (relativistic Döppler effect)

$$h\nu' = h\nu\gamma(1 - \underline{\beta}\cdot\underline{e}_k) \tag{1}$$

where $\underline{\beta}$ is the velocity of the proton, $\underline{e}_k$ is the direction of

* Corresponding author.
E-mail address: camilla.curatolo@mi.infn.it (C. Curatolo).

http://dx.doi.org/10.1016/j.nima.2016.09.002

Please cite this article as: C. Curatolo, et al., Nuclear Instruments & Methods in Physics Research A (2016), http://dx.doi.org/10.1016/j.nima.2016.09.002

Table 1
Particles properties (case LHC). Values of momenta in [GeV/c], angles in [μrad].

Particle	p_z^{min} [GeV/c]	p_z^{max} [GeV/c]	p_x^{max} [GeV/c]	θ^{rms} [μrad]
Proton	≃7000	7000	0.187	27
Photon	20 keV	20 keV	0	0
Pion	260	2540	0.38	145
Neutron	4450	6740	0.38	27
Muon	149	2500	0.38	147
Neutrino	0	1080	0.16	≤500

propagation of the photon, $\gamma = E_p/M_p$ and $M_p = 938$ MeV/c^2. For an ultra-relativistic proton colliding head-on with a photon, the formula simplifies in $h\nu' \simeq 2\gamma h\nu$. The energy E_{CM} available in the center of mass (CM) of the proton–photon system is

$$E_{CM} = \sqrt{P^2} = \sqrt{2E_p h\nu - 2(\underline{p}_p \cdot \underline{k}) + M_p^2} \tag{2}$$

where $P = \{E_p + h\nu, \underline{p}_p + \underline{k}\}$. Assuming $h\nu \ll E_p$,

$$\gamma_{CM} = \frac{E_{tot}^{LAB}}{E_{CM}} \simeq \frac{E_p + h\nu}{\sqrt{4E_p h\nu + M_p^2}}. \tag{3}$$

Once we define the parameter representing the recoil of the proton in the collision as $\Delta_p \equiv 4\gamma h\nu/M_p$, we can write $E_{CM} \simeq M_p\sqrt{1+\Delta_p}$ and $\gamma_{CM} \simeq \gamma/\sqrt{1+\Delta_p}$. We discuss in the following the pion photoproduction and its decay into muon and neutrino and the direct muon pair photoproduction by showing some of the results obtained by a home made event generator. Natural units $c = \hbar = 1$ have been adopted and $_*$ denotes the particles' momenta and energies in their CM reference frame.

2.1. Muon production through pion production

The threshold for the $p + h\nu \to \pi^+ + n$ reaction is set by $p_\pi^* = p_n^* = 0$, corresponding to $\Delta_p^{th} = (M_\pi + M_n)^2/M_p^2 - 1 = 0.324$ (since $E_{CM}^{th} = M_p\sqrt{1+\Delta_p^{th}} = M_\pi + M_n$) and a photon minimum energy $h\nu^{th} = M_p\Delta_p^{th}/4\gamma \simeq 76[\text{MeV}]/\gamma$, equivalent to $h\nu'^{th} = 152$ MeV seen by the proton. In order to evaluate the emittance of the generated pion beam it is useful to consider the first order behavior of momentum in CM just above threshold, i.e.

$$p_\pi^{*th} = p_n^{*th} \simeq \frac{M_p}{2}\sqrt{1 - \frac{(M_\pi^2 - M_n^2)^2}{(M_\pi^2 + M_n^2)^4}}\sqrt{\Delta_p - \Delta_p^{th}}. \tag{4}$$

The transverse momenta are invariant to Lorentz transformations along the perpendicular direction from CM to LAB frames, therefore the normalized transverse emittance of the pion beam at the interaction point is

$$\epsilon_n^{\pi_x} = \frac{\sigma_0}{\sqrt{2}}\sqrt{\langle \overline{p}_{\pi_x}^2 \rangle} \tag{5}$$

where $\overline{p}_{\pi_x} \equiv p_{\pi_x}/M_\pi$, the average is performed over the phase space distribution area and σ_0 is the proton beam spot size at the interaction point. The factor $1/\sqrt{2}$ represents the emitted beams rms spot size decrease: in this case we assumed a perfect overlap of the two Gaussian colliding beams with the same spot size σ_0. The thermal normalized emittance of the pion beam, due to the collision transverse temperature, is

$$\epsilon_{n-cath}^{\pi_x} = \frac{2.25}{\sqrt{3}}\frac{\sigma_0}{\sqrt{2}}\sqrt{\Delta_p - 0.324} \tag{6}$$

assuming a uniform distribution of momenta in the transverse phase space. By evaluating the difference between maximum

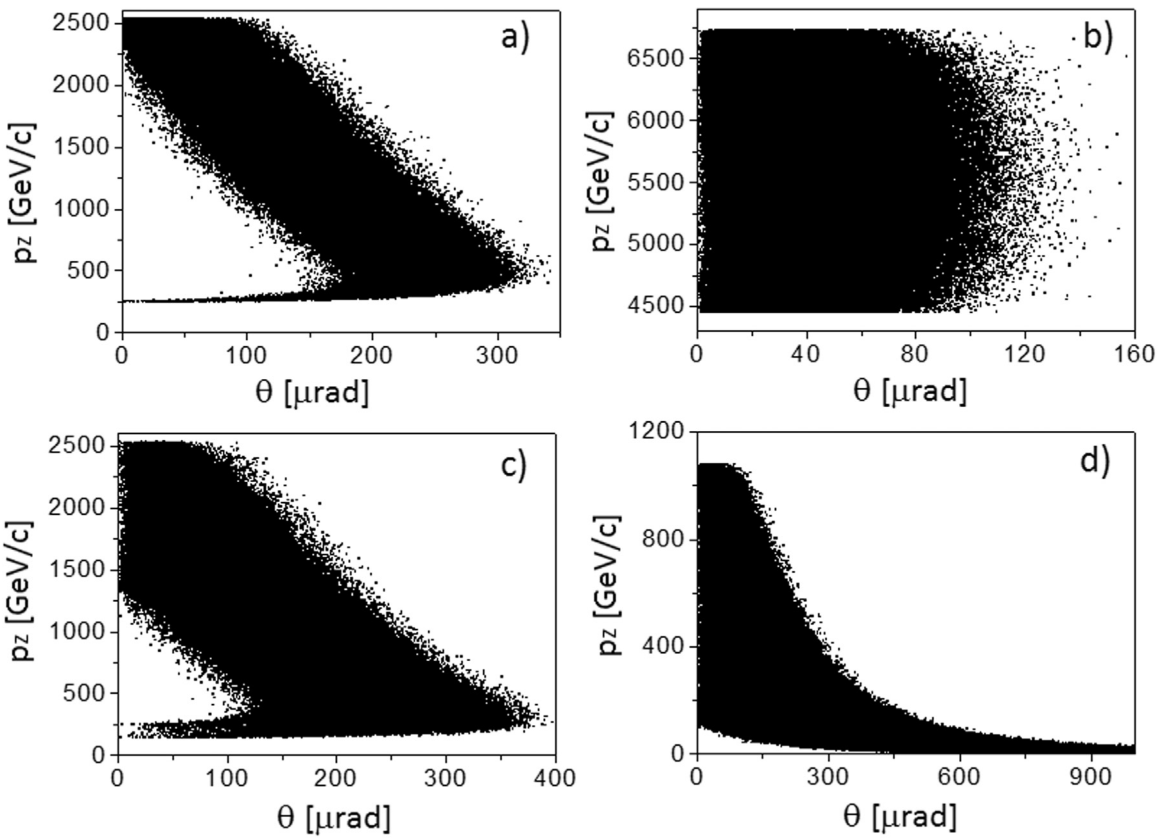

Fig. 1. Pions (a), neutrons (b), muons (c) and neutrinos (d) longitudinal momentum [GeV/c] as a function of θ [μrad] (case LHC).

Please cite this article as: C. Curatolo, et al., Nuclear Instruments & Methods in Physics Research A (2016), http://dx.doi.org/10.1016/j.nima.2016.09.002

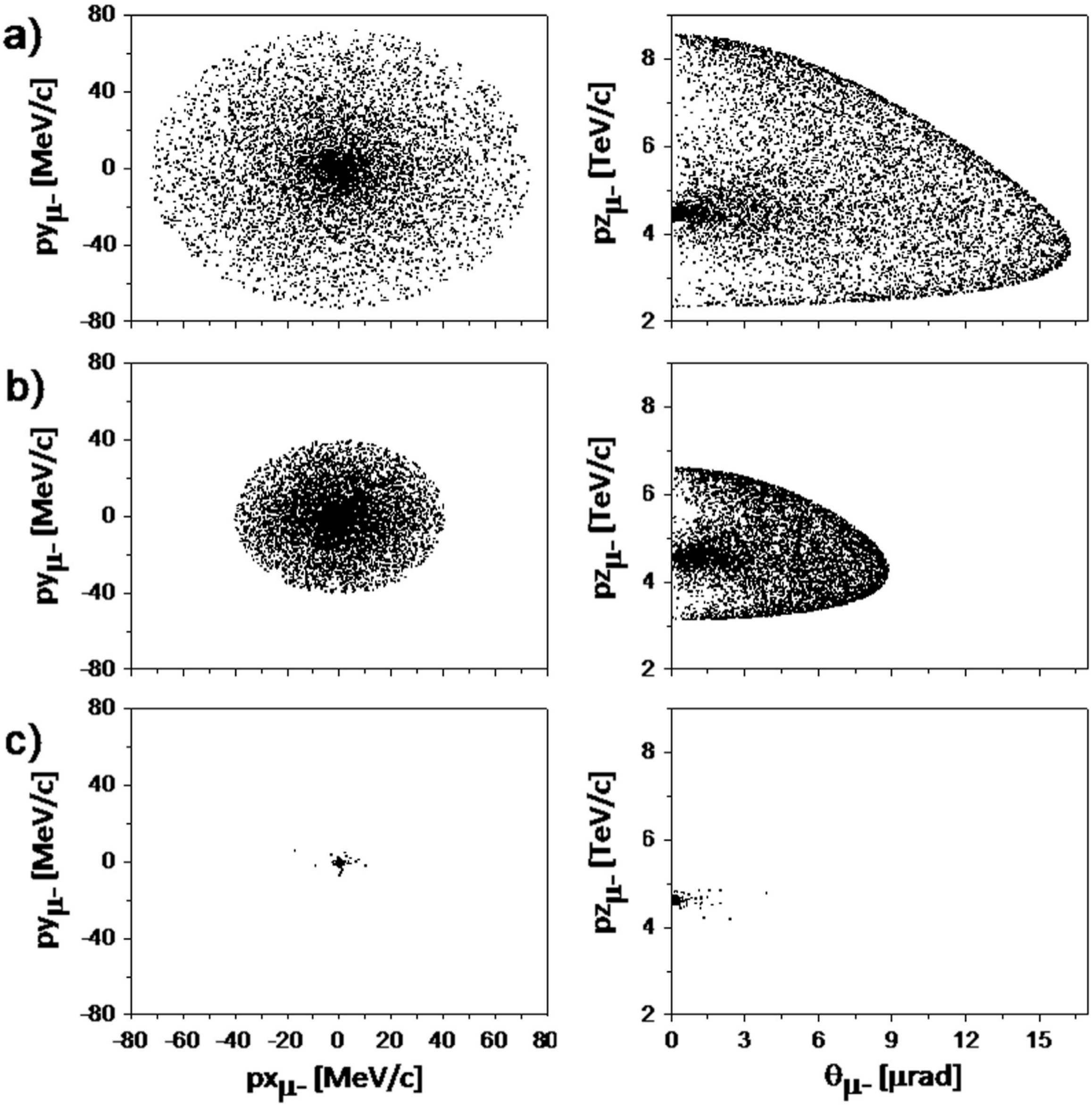

Fig. 2. Features of the $\mu-$ beam at different values of the photon energy $h\nu = 2.5$ (a), 2.3 (b) and 2.2053 (c) keV, without considering the emittance of the proton beam at $E_p = 50$ TeV.

$p_{\pi_z}(\theta^* = 0)$ and minimum $p_{\pi_z}(\theta^* = \pi)$ pion momentum in LAB, we derive the rms energy spread of the pion beam as

$$\frac{\Delta\gamma}{\gamma}_{\pi} = \frac{M_p}{2\sqrt{3}M_\pi}\sqrt{1 - \frac{(M_\pi^2 - M_n^2)^2}{(M_\pi^2 + M_n^2)^4}}\sqrt{\Delta_p - 0.324} \tag{7}$$

for a uniform longitudinal momentum distribution.

The mean life-time of a pion at rest in the laboratory frame is $\tau_\pi = 2.6 \cdot 10^{-8}$ s to decay into a muon and a neutrino according to $\pi^+ \to \mu^+ + \nu_\mu$. In our case the pion mean life-time is $\gamma_\pi \cdot \tau_\pi$, which implies pions propagating over long distances (hundred meters to several kms). In the following we will populate the phase space volumes of the generated pion and muon beams neglecting effects coming from this long range pion propagation: the reason for this assumption is to focus the present analysis on the secondary beam generation process and leaving to a future work the study about matching the generated beams into a further storage/acceleration stage.

We create an event-generator code to simulate the $p + h\nu \to \pi^+ + n$ and $\pi^+ \to \mu^+ + \nu_\mu$ reactions. As an example we report the results obtained for $E_p = 7$ TeV and $h\nu = 20$ keV (case LHC): the protons are distributed in a circle of 10 μm radius ($\sigma_0 = 7$ μm) and the scattering angle θ in LAB is taken with respect to the mean direction of the proton beam propagation. The FEL photon beam diffraction has been disregarded and we supposed an optimal space-time overlap between the two colliding beams at the IP, i.e. $\sigma_0 = \sigma_{h\nu_x}$. We take into account the effect of the proton beam transverse emittance, which spreads the protons transverse momentum in phase space according to equation $\sigma_{p_{p_x}} \equiv M_p\sqrt{\langle \overline{p}_{p_x}^2 \rangle} = M_p\epsilon_n^{p_x}/\sigma_0$, where $\sigma_{p_{p_x}}$ is the rms proton beam transverse momentum. The minimum and maximum value of the longitudinal momentum, the maximum value of p_x and of θ are reported in Table 1 and the angle-energy dependence is shown in Fig. 1 for all the kind of particles involved in the reaction. The pion beam transverse emittance is 3.88 mm mrad while the muons' is 4.14 mm mrad. As we see in Fig. 1, at the same angle in the laboratory frame we can find the same kind of particle at very different energies, therefore an eventual selection has to be performed in the terms of energy.

Please cite this article as: C. Curatolo, et al., Nuclear Instruments & Methods in Physics Research A (2016), http://dx.doi.org/10.1016/j.nima.2016.09.002

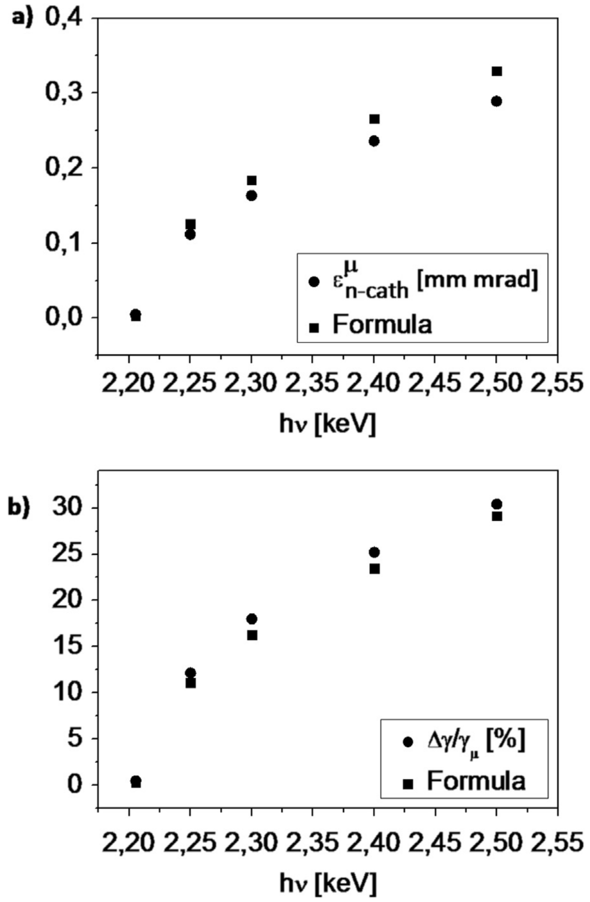

Fig. 3. Graph a): Simulated emittance of μ^- beam (dots) and Formula (8) (squares) as a function of $h\nu$ [keV]. Graph b): Relative energy spread of $\mu-$ beam [%] (dots) and Formula (9) (squares) vs photon energy [keV]. No proton beam emittance.

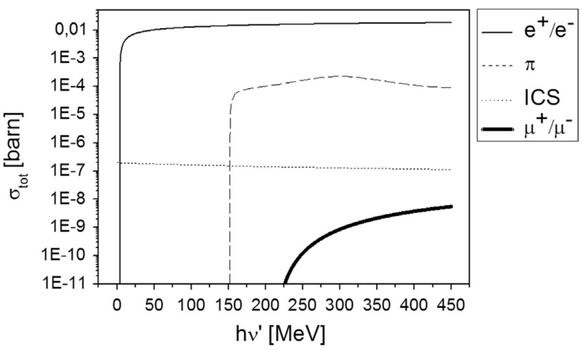

Fig. 4. Total cross section σ_{tot} in [barn] as a function of the photon energy $h\nu'$ [MeV] for different reactions: electron/positron (solid thin line), pion (dashed line), inverse Compton scattering (dotted line) and muon pair (solid thick line) photoproduction [9,10].

Table 2
Number of particles [s^{-1}] at $E_p = 50$ TeV and $h\nu$ [keV] values reported in table.

E_p [TeV]	$h\nu$ [keV]	N_π [s^{-1}]	N_μ [s^{-1}]	N_e [s^{-1}]
50	1.43 (πth)	$1.86\cdot10^{10}$	0	$4.5\cdot10^{12}$
50	2.2053 (μth)	$3.72\cdot10^{10}$	$1.25\cdot10^{4}$	$5\cdot10^{12}$
50	3	$6.5\cdot10^{10}$	$4\cdot10^{5}$	$5.4\cdot10^{12}$

2.2. Direct muon pair production

Let us now consider the direct muon pair production via $p + h\nu \rightarrow p' + \mu^-\mu^+$. Fig. 2 shows the phase spaces of the muon produced by the collision of protons at $E_p = 50$ TeV and photons at different energies around the threshold value.

The thermal normalized emittance of the muon beams, due to the collision transverse temperature, can be written as

$$\epsilon^{\mu}_{n-cath} \le \frac{1}{\sqrt{3}}\frac{\sigma_0}{\sqrt{2}}\sqrt{\frac{M_p^2}{4M_\mu^2}\left(\sqrt{1+\Delta_p}-1\right)^2-1} \tag{8}$$

where σ_0 is the proton beam spot size at the interaction point (assuming a uniform distribution of momenta in the transverse phase space of the muon beams). The values of the normalized transverse emittance for $E_p = 50$ TeV and several photon energies are reported in Fig. 3a): the emittance in this cases is purely thermal (no proton beam emittance). The simulated values (dots) are compared to the ones given by Formula (8) (squares). In case the proton beam emittance is considered, the total transverse normalized emittance ϵ^μ is such that $\epsilon_1 < \epsilon_n^\mu < \epsilon_2$ where $\epsilon_1 = \sqrt{(\epsilon^{\mu}_{n-cath})^2 + (\epsilon_n^{p'})^2}$ and $\epsilon_2 = \epsilon^{\mu}_{n-cath} + \epsilon_n^{p'}$. We can evaluate the rms energy spread of the muon beams as

$$\frac{\Delta\gamma}{\gamma}_{\mu} = \frac{1}{\sqrt{3}}\sqrt{\frac{M_p^2}{4M_\mu^2}\left(\sqrt{1+\Delta_p}-1\right)^2-1}\,. \tag{9}$$

The simulated relative energy spread values are reported in Fig. 3b) (dots) in comparison to the values of the analytical expression (9) (squares).

3. Luminosity and flux

At each collision, the number of a certain kind of particle produced can be calculated as

$$\mathcal{N} = \mathcal{L}\cdot\Sigma = \frac{N_p N_{ph} r}{4\pi\sigma_0^2}\cdot\Sigma \tag{10}$$

where Σ is the total cross section for the considered reaction, $\mathcal{L}$ is the proton–photon collider luminosity, N_p is the number of colliding protons in the bunch, N_{ph} is the number of photons carried by the radiation pulse, r the repetition rate of the collisions and σ_0 the effective spot size at the IP. Since the interaction does not produce beam-beam effects, we can assume that the geometrical luminosity considered in Eq. (10) is a good assumption as far as the hour-glass effects are negligible. Concerning the maximum repetition rate achievable in collisions, LHC can be operated up to 40 MHz and FCC is expected to match it, while XFEL based on SC CW Linacs are aimed at achieving 1 MHz, but the upgrade to 10 MHz is considered feasible by adopting Energy Recovery Linacs schemes. Besides the pion and the direct muon pair photoproduction, the main reactions in the energy range $100\text{ MeV} < h\nu' < 400\text{ MeV}$ are electron-positron pair production and inverse Compton scattering. The total cross sections are summarized in Fig. 4. Considering an FCC beam of $N_{pr} = 10^{11}$ and $\sigma_0 = 1.6\ \mu$m, $N_{ph} = 10^{14}$ and $r = 10$ MHz, we obtain a luminosity of $\mathcal{L} = 3.1\cdot10^{38}\ cm^{-2}\,s^{-1}$ and the expected number of events per second are specified in Table 2.

4. Conclusion

The combined operation of LHC/FCC with a X-ray Free Electron Laser, although not easy nor inexpensive to be implemented in

Please cite this article as: C. Curatolo, et al., Nuclear Instruments & Methods in Physics Research A (2016), http://dx.doi.org/10.1016/j.nima.2016.09.002

reality, offers the great opportunity of conceiving a hybrid HPC, at an unprecedented luminosity exceeding $10^{38}\ s^{-1}\ cm^{-2}$. The HPC is actually aimed not at producing events to study, but to generate secondary beams of unique characteristics, via a highly boosted Lorentz frame corresponding to a very relativistic moving center of mass reference frame. The phase space distributions of the secondary beam generated, in particular pions, have outstanding properties of low transverse emittance (in the range 3 – 5.5 mm mrad) and are collimated within very narrow forward angles (less than 150 μrad for a 7 TeV colliding proton beam as for LHC and less 10 μrad for a 50 TeV proton beam as for FCC) with energies attaining 2.5 TeV and 19.1 TeV respectively for the two cases (LHC and FCC) [11,12]. The opportunity consists in conceiving a beam manipulation of charged pions of both signs, generated in the HPC, capable to let them decay into muons and neutrino beams of similar characteristics in the phase space: the challenge is the large energy spread of the pion beams (an energy selection will have to be implemented first) and the long range distance travelled by them before decay, at this energy. The potentialities in terms of muon and neutrino beams obtainable are impressive: although the number of muons and neutrinos per bunch would be low (a few thousands) their phase space distributions would be extremely high quality thanks to the large Lorentz boost of the primary proton-photon collision, giving rise to very small divergence angles for these beams. Another way to obtain muon beams is the direct muon pair production: despite the very low cross section value, the critical steps represented by the production of charged pions of both signs and the storage and selection of the pions would be overcome. A possibility to partially compensate for the low efficiency of the process would be to collide lead ions in order to have a factor ~670 gain on the number of produced muons: around 10^8 muon pairs per second. In both scenarios, the long life of the high energy generated muons (in excess of 10 ms) may offer the opportunity to accumulate them in a storage ring so to achieve muon collider requested bunch intensities.

References

[1] D. Neuffer, M. Palmer, Y. Alexahin, C. Ankenbrandt, J. Delahaye, A Muon Collider as a Higgs Factory, arXiv:hep-ex/0207031v3, 2015.

[2] D.M. Kaplan, Muon Colliders and Neutrino Factories, arXiv:1412.3487v1, 2014.

[3] C.M. Ankenbrandt, et al., Status of muon collider research and development and future plans, Phys. Rev. ST Accel. Beams 2 (1999) 081001, http://dx.doi.org/10.1103/PhysRevSTAB.2.081001 arXiv:physics/9901022.

[4] M.M. Alsharo'a, Recent Progress in Neutrino Factory and Muon Collider Research within the Muon Collaboration, arXiv:hep-ex/0207031v3, 2003.

[5] E. Todesco, F. Zimmermann, The higher-energy large hadron collider, in: Proceedings of EuCARD-AccNet HE-LHC Workshop, 2010.

[6] Future Circular Collider, ⟨https://fcc.web.cern.ch/Pages/default.aspx⟩, 2015.

[7] C. Emma, J. Wu, K. Fang, S. Chen, S. Serkez, C. Pellegrini, Terawatt x-ray free-electron-laser optimization by transverse electron distribution shaping, Phys. Rev. ST Accel. Beams 17 (2014) 110701, http://dx.doi.org/10.1103/PhysRevSTAB.17.110701.

[8] I. Agapov, Sase characteristics from baseline European XFEL undulators in the tapering regime, in: Proceedings of FEL2014, Basel, Switzerland, 2014, MOP056.

[9] D. Drechsel, L. Tiator, Threshold pion photoproduction on nucleons, J. Phys. G18 (1992) 449–497, http://dx.doi.org/10.1088/0954-3899/18/3/004.

[10] J.W. Motz, H.A. Olsen, H.W. Koch, Pair production by photons, Rev. Mod. Phys. 41 (1969) 581–639, http://dx.doi.org/10.1103/RevModPhys.41.581.

[11] L. Serafini, C. Curatolo, V. Petrillo, Low Emittance Pion Beams Generation from Bright Photons and Relativistic Protons, arXiv:1507.06626v2, 2015.

[12] C. Curatolo, PhD Thesis: High brilliance photon pulses interacting with relativistic electron and proton beams, ⟨https://air.unimi.it/handle/2434/358227⟩, 2016.

Please cite this article as: C. Curatolo, et al., Nuclear Instruments & Methods in Physics Research A (2016), http://dx.doi.org/10.1016/j.nima.2016.09.002